An Age-Structured Vaccination Strategy for Epidemic Containment: A Model Predictive Control Approach

Candy Sonveaux[1], Morgane Dumont*[2], Mirko Fiacchini[3], and Mohamad Ajami[3]

[1]University of Namur, Department of Mathematics and naXys, Belgium
[2]QuantOM, HEC - Management School of the University of Liège, Belgium,
[3] Univ. Grenoble Alpes, CNRS, Grenoble INP, GIPSA-lab, Grenoble, France

February 10, 2026

Abstract

This work presents a novel Model Predictive Control (MPC) approach to develop an optimal age-structured vaccination strategy for the containment of COVID-19 in Wallonia, Belgium. The proposed MPC framework is designed to minimize deaths, achieve early disease eradication, and adhere to operational constraints. By incorporating an age-structured Susceptible-Infected-Recovered-Deceased (SIRD) model with an additional term for vaccination, the MPC strategy dynamically adapts to the evolving epidemic state. A detailed proof of the asymptotic stability and recursive feasibility of the proposed MPC algorithm is provided. This ensures that the optimal cost at each step provides an upper bound on the minimal number obtainable of deaths at the end of the pandemic. Moreover, simulations demonstrate that the proposed MPC approach outperforms the decreasing age vaccination strategy adopted by the Belgian government during the first wave of vaccinations. The results highlight the potential of MPC-based vaccination strategies to reduce the total number of deaths, accelerate disease eradication, and optimize vaccine administration.

Keywords: Model predictive control Epidemic control Asymptotic stability Vaccination strategy optimization

1 Introduction

Over the last decades, the number of major epidemics and pandemics has increased significantly. An epidemic can be defined as the widespread outbreak of an infectious disease in a community at a particular time. A pandemic is an epidemic that spreads across different regions. Throughout history, epidemics and pandemics have shown their ability to claim countless lives and exhaust healthcare systems. One can cite the Ebola virus disease that occurred in West Africa between 2014 and 2016 and more recently the COVID-19 pandemic. Until the 5^{th} of January, 2025, more than 7 million lives have been lost to COVID-19 according to [World Health Organization, 2025], with half of these deaths occurring during the first year of the pandemic. This highlights the need for reliable and cost-effective strategies that would enable nations, regardless of their economic power, to combat spread and save as many lives as possible.

According to the objectives of the World Health Organization, [World Health Organization, 2014], immediate action is required once an epidemic emerges, since the disease is already circulating by the time it is detected. Hence, scientists and decision makers must unite their efforts to develop and enforce measures to control spread without crippling the economy. In the early stages of an epidemic, scientists focus on rapidly testing and developing vaccines, while decision makers enforce regulations to limit transmission. Once vaccines become available, decision makers deploy vaccination strategies to effectively contain the outbreak.

*corresponding author : morgane.dumont@uliege.be

Decision makers often use mathematical models to support their decisions. Compartmental models in epidemiology divide the population under study into disjoint compartments, each representing a certain disease status, referred to as states [Brauer, 2008]. These models describe how the population dynamically evolves between states over time. In [Tolles and Luong, 2020], the authors present a comprehensive overview of compartmental models in epidemiology. The first known compartmental model is the SIR model [Kermack and McKendrick, 1991], which consists of three compartments: Susceptible individuals (S) who can contract the disease, Infected individuals (I) who can transmit the disease, and Recovered individuals (R) who are assumed to be immune against the disease. Depending on the objectives of the study and the complexity of the disease, additional compartments may be added. However, increasing the complexity of the model can lead to problems of identifiability and forecasting capability [Fiacchini and Alamir, 2021].

In this paper, an age-dependent vaccination strategy based on Model Predictive Control (MPC) is proposed. The strategy is applied to COVID-19 data for Wallonia, Belgium. The MPC employs an age-structured SIRD model that incorporates an additional compartment describing the total number of Deceased individuals (D). An additional input term for vaccination is included in the model to study the impact of vaccine administration on population dynamics. Although the traditional SIRD model does not consider age, the age-dependent nature of COVID-19 requires models that take into account the demographic factor. In fact, parameters such as death and recovery rates have been shown to be age-dependent [Davies et al., 2020]. In addition, similar models have been adopted in the literature to develop strategies against pandemics. In [Grundel et al., 2022], a social distancing strategy is developed to achieve the containment of COVID-19. In Belgium, several studies were aimed at developing variants of the SIRD model. In [Franco, 2021], the authors present an age-structured SEIR-QD model (Susceptible-Exposed-Infectious-Recovered-Quarantined-Deceased) that includes nursing home dynamics to forecast the progression of COVID-19 and assess the effects of long-term public health strategies. In [Alleman et al., 2021], a social contact model integrates public mobility data to evaluate the impact of non-pharmaceutical interventions on virus transmission in different settings. A similar model is used in [Abrams et al., 2021] to analyze the effects of early lockdown on hospitalizations and project future epidemic scenarios based on various exit strategies. To our knowledge, no study has proposed a dynamic framework to guide the COVID-19 vaccination strategy using an age-stratified SIRD model, accompanied by a stability and recursive feasibility proof.

Model predictive control for strategic epidemic planning has been extensively examined in the literature. In [Morato et al., 2020], an MPC is developed to adapt the social distancing policies for COVID-19. Moreover, in [Grundel et al., 2022], the authors used an SIRD model within an MPC framework to optimize mass testing and develop an age-specific social distancing strategy. Similarly, the authors in [Sauerteig et al., 2022] introduced an MPC approach using an age-independent SEIR model to minimize social distancing and quarantine measures during a pandemic while maintaining a strict infection cap. On the other hand, the authors in [Parino et al., 2023] developed an age-dependent MPC two-dose scheduling strategy for COVID-19 vaccine administration to balance health requirements and socioeconomic costs. Furthermore, a vaccination strategy is proposed in [Cartocci et al., 2021], with given objectives such as minimizing total infections, total deaths, and total quality adjusted life years (QALY). However, exhaustive full-grid simulations were performed in that study without providing any guarantee on the obtained solution. A proof of recursive feasibility and asymptotic convergence is crucial even for inherently stable systems, as the case of pandemic dynamics, since it also provides guaranteed bounds on the infinite-horizon optimal solution.

To date, there has been no consensus on the definition of an optimal vaccination strategy. For example, Belgium adopted a decreasing-age vaccination strategy, starting with the elderly. The argument was that COVID-19 posed a higher mortality risk in older age groups compared to younger ones. In contrast, [Rahmandad, 2022] argues that it is more effective to base the vaccination strategy on the level of contact, suggesting that the level of exposure is more critical than age to eradicate the disease as quickly as possible. This dilemma raises the need for a dynamic framework to guide the vaccination strategy in an optimal manner. This work proposes a novel age-structured MPC approach to design a vaccination strategy aimed at minimizing fatalities. A proof of asymptotic stability and recursive feasibility of the proposed algorithm is provided, ensuring that the final death toll minimization is upper bounded by the MPC cost.

This paper is organized as follows: Section 2 presents the epidemiological model used in this study, detailing the age-structured SIRD model and its parameters. Section 3 introduces the Model Predictive

Control (MPC) framework, including the proof of recursive feasibility and asymptotic stability. Section 4 discusses the implementation of the MPC-based vaccination strategy for COVID-19 in Wallonia and compares its performance with the Belgium national vaccination strategy through simulations. Finally, Section 5 concludes the paper by summarizing the key findings and suggesting directions for future research.

2 Epidemiological Model

This work focuses on an age-structured Susceptible-Infected-Recovered-Deceased (SIRD) model with an additional input term for vaccination. This model is used to analyze the impact of the administration of the COVID-19 vaccine on the dynamics of the Walloon population. Compartmental models, such as the SIRD model, are widely utilized in the literature to study the effects of various epidemic containment measures on population dynamics. This section provides a comprehensive overview of the model structure and parameters. The continuous-time SIRD model is presented in (1) as follows:

$$\begin{cases} \dfrac{dS_k(t)}{dt} = -\lambda_k S_k(t) \displaystyle\sum_{j=1}^{n_a} C_{kj} I_j(t) - u_k(t) \\ \dfrac{dI_k(t)}{dt} = \lambda_k S_k(t) \displaystyle\sum_{j=1}^{n_a} C_{kj} I_j(t) - (\gamma_{R_k} + \gamma_{D_k}) I_k(t) \\ \dfrac{dR_k(t)}{dt} = \gamma_{R_k} I_k(t) + u_k(t) \\ \dfrac{dD_k(t)}{dt} = \gamma_{D_k} I_k(t) \end{cases} \tag{1}$$

where $S_k(t)$, $I_k(t)$, $R_k(t)$, and $D_k(t)$ denote the number of susceptible, infected, recovered, and deceased individuals, respectively, in the k^{th} age group, with $k \in \{1, 2, \ldots, n_a\}$, at time t; n_a is the total number of considered age groups. The term λ_k represents the probability of disease transmission when an individual in the k^{th} age group has a contact. The term C_{ij} represents the probability that an individual in the i^{th} age group encounters someone in the j^{th} age group. The parameters γ_{R_k} and γ_{D_k} refer to the recovery and death rates, respectively, for the k^{th} age group. The input $u_k(t)$ is defined as the vaccination rate among susceptible individuals in the k^{th} age group at time t. Figure 1 provides a graphical representation of the continuous-time SIRD model in (1) for the k^{th} age group. The total population considered in the model is assumed to be constant, as derived from the model equations, where the sum of the derivatives of the compartments, representing the derivative of the total population, is zero.

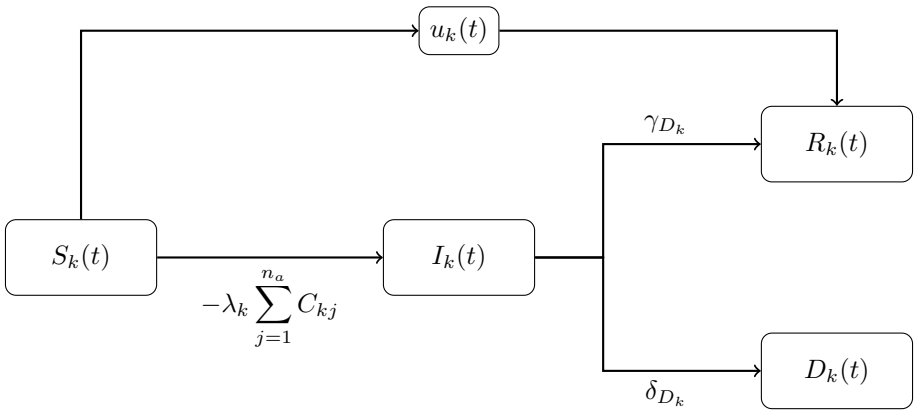

Figure 1: Compartmental scheme of the age-structured SIRD model with an additional vaccination term for the k^{th} age group

In the context of Model Predictive Control, the continuous-time model in (1) is discretized using the Forward Euler Method to account for the discrete-time nature of the optimization problem. To

align with the frequency of data updates and the meeting of decision makers, the model is discretized at a sampling time $ts = 1$ (in *days*). The discrete-time age-structured SIRD model is represented in (2) as follows:

$$\begin{cases} S_k(n+1) = S_k(n) - \lambda_k S_k(n) \sum_{j=1}^{n_a} C_{kj} I_j(n) - u_k(n) \\ I_k(n+1) = I_k(n) + \lambda_k S_k(n) \sum_{j=1}^{n_a} C_{kj} I_j(n) - (\gamma_{R_k} + \gamma_{D_k}) I_k(n) \\ R_k(n+1) = R_k(n) + \gamma_{R_k} I_k(n) + u_k(n) \\ D_k(n+1) = D_k(n) + \gamma_{D_k} I_k(n) \end{cases} \tag{2}$$

Here, $n \in \mathbb{N}$ represents the discrete-time step, where each n corresponds to the n^{th} day since the beginning of the COVID-19 outbreak.

3 Model Predictive Control

The primary goal of this work is to prove that for complex dynamics and objectives, such as finding the best vaccination strategy for the COVID-19 pandemic, optimization-based methods might outperform alternative approaches, based on the intuition, which could fail to capture the inherent complexity of the problem. To fulfill it, an optimal age-dependent vaccination strategy, based on model predictive control, is proposed to minimize the final deaths toll and eradicate disease while adhering to operational constraints. MPC operates by minimizing a predefined cost over a finite time horizon, called the prediction horizon N, at every sampled instant; see the schematic illustration in Figure 2. The plant model is used to forecast the future trajectories of the system and select the optimal one. From the calculated solution, only the first control action is used and the process is repeated for the next time step. This iterative nature of the MPC enables it to predict, anticipate, and adapt to changing conditions.

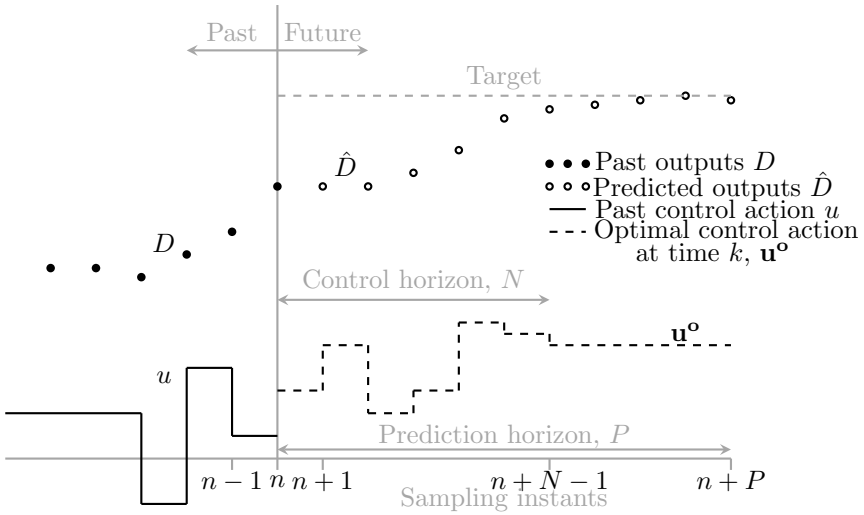

Figure 2: Illustration of the MPC scheme, inspired by [Seborg et al., 2016]

Moreover, this work provides proofs of the recursive feasibility and asymptotic stability of the problem. In general, the conditions for them to hold are already well established in the literature. However, ensuring their satisfaction for nonlinear systems is not straightforward, in general. It is important to recall that, even for inherently asymptotically stable systems, a proof of recursive feasibility and asymptotic stability is fundamental since it provides bounds on the optimal infinite-horizon solution attainable. In particular, the resulting optimal cost provides an upper bound on the minimal final number of deaths obtainable at the end of the vaccination procedure.

3.1 Recursive feasibility and stability conditions for general MPC

Before proceeding to design the MPC-based vaccination strategy, some general theoretical results are recalled. The proof of recursive feasibility and asymptotic stability is achieved by introducing notations from the classical MPC theory in [Rawlings et al., 2017]. Consider the general dynamical system given by:

$$x(n+1) = f(x(n), u(n)), \quad \text{with} \quad x(0) = x_0 \tag{3}$$

where $x \in \mathbb{X}$ is the current state, $u \in \mathbb{U}$ is the current control action, and f is a non-linear function that describes the evolution of the next state. The sets $\mathbb{X}$ and $\mathbb{U}$ represent the state and input constraints. In what follows, the order operators (i.e. $<, \leq$, etc.) are considered to be elementwise when applied to vectors.

The proofs of recursive feasibility, asymptotic convergence of the closed-loop solution, and the upper bound on the future death toll are based on standard results from the classical MPC theory. The general form of the MPC is structured as follows:

$$\begin{aligned} \mathbb{P}_N(x): \quad & \min_{\mathbf{u}} V_N(x, \mathbf{u}) \\ \text{s.t.} \quad & x(n+1) = f(x(n), u(n)), \quad \forall n \in \{0, 1, \ldots, N-1\}, \\ & x(0) = x, \\ & (x(n), u(n)) \in \mathbb{Z}, \quad \forall n \in \{0, 1, \ldots, N-1\}, \\ & x(N) \in \mathbb{X}_f \subseteq \mathbb{X}. \end{aligned} \tag{4}$$

with

$$V_N(x, \mathbf{u}) = \sum_{n=0}^{N-1} l(x(n), u(n)) + V_f(x(N)) \tag{5}$$

where $N \in \mathbb{N}$ is the prediction horizon, $\mathbb{Z}$ is a subset of $\mathbb{X} \times \mathbb{U}$ representing the constraints on future trajectories, and $\mathbb{X}_f$ and $V_f(\cdot)$ are additional parameters designed to ensure stability and recursive feasibility properties. The performance cost to be minimized at each step, $V_N(x, \mathbf{u})$, represents the total cost over the prediction horizon, where $l(x(n), u(n))$ is a function that captures the stage cost at time n and $V_f(x(N))$ is the terminal cost.

By defining $\mathcal{U}_N(x) \in \mathbb{U}^N$ as the set of feasible control sequences that satisfy the input, state and terminal constraints of problem (4) at x, the optimal control problem can be rewritten as:

$$\mathbb{P}_N(x): \min_{\mathbf{u} \in \mathcal{U}_N(x)} V_N(x, \mathbf{u}) := V_N^0(x). \tag{6}$$

Moreover, the feasibility region of the problem, i.e. the subset of $\mathbb{X}$ where (4) admits a solution, is denoted as $\mathcal{X}_N$, that is $\mathcal{X}_N = \{x \in \mathbb{X} : \mathcal{U}_N(x) \neq \emptyset\}$. The optimal control sequence $\mathbf{u}^0(x)$ can hence be obtained by solving the optimal control problem in (6), which yields the following:

$$\mathbf{u}^0(x) = (u^0(0, x), \ldots, u^0(N-1, x)) = \arg \min_{\mathbf{u} \in \mathcal{U}_N(x)} V_N(x, \mathbf{u})$$

where only the first element of the input sequence $\kappa_N(x) = u^0(0, x)$ is used to control the system. The classical proof that guarantees closed-loop recursive feasibility and asymptotic stability of the system using MPC, see Theorem 2.19 in [Rawlings et al., 2017], is recalled hereafter.

Theorem 1 ([Rawlings et al., 2017]) *Given the dynamical system (3), the optimization problem (4) and the equilibrium set $X^* \subseteq \mathbb{X}$, suppose that:*

1. *the functions $f : \mathbb{Z} \to \mathbb{X}$, $l : \mathbb{Z} \to \mathbb{R}_+$ and $V_f : \mathbb{X} \to \mathbb{R}_+$ are continuous;*
2. *$f(x^*, 0) = 0$, $l(x^*, 0) = 0$ and $V_f(x^*, 0) = 0$ $\forall x^* \in X^*$;*
3. *the set $\mathbb{Z}$ is closed, $\mathbb{X}_f \subseteq \mathbb{X}$ is compact, $X^* \subseteq \mathbb{X}_f$, and $0 \in \mathbb{U}$, where $\mathbb{U}$ is compact;*
4. *for every $x \in \mathbb{X}_f$, there exists $u \in \mathbb{U}$, such that $(x, u) \in \mathbb{Z}$ and:*
   (a) *$f(x, u) \in \mathbb{X}_f$,*

(b) $V_f(f(x,u)) - V_f(x) \leq -l(x,u)$;

5. *there exist two* $\mathcal{K}_\infty$ *functions,* $\alpha_1(\cdot)$ *and* $\alpha_f(\cdot)$*, satisfying:*

   (a) $l(x,u) \geq \alpha_1(\|x\|_{X^*}), \quad \forall x \in \mathcal{X}_N, \forall u$ *such that* $(x,u) \in \mathbb{Z}$,

   (b) $V_f(x) \leq \alpha_f(\|x\|_{X^*}), \quad \forall x \in \mathbb{X}_f$, *with* $\|x\|_{X^*} := \min_{x^* \in X^*} \|x - x^*\|$;

6. *there exists a* $\mathcal{K}_\infty$ *function* $\alpha(\cdot)$ *such that* $V_N^0(x) \leq \alpha(\|x\|_{X^*})\ \forall x \in \mathcal{X}_N$.

Then, the optimal control problem in (4) is feasible $\forall x \in \mathcal{X}_N$*, and there exist two* $\mathcal{K}_\infty$ *functions:* $\alpha_d(\cdot)$ *and* $\alpha_u(\cdot)$*, such that* $\forall x \in \mathcal{X}_N$*,*

$$\alpha_d(\|x\|_{X^*}) \leq V_N^0(x) \leq \alpha_u(\|x\|_{X^*}),$$
$$V_N^0(f(x, \kappa_N(x)) - V_N^0(x) \leq -\alpha_d(\|x\|_{X^*}),$$

and hence $V_N^0(\cdot)$ *is a Lyapunov function defined in* $\mathcal{X}_N$*. Therefore, the set* X^* *is asymptotically stable in* $\mathcal{X}_N$ *for* $x(n+1) = f(x(n), \kappa_N(x(n)))$.

The recursive feasibility and asymptotic convergence of the proposed MPC vaccination approach can be ensured by satisfying the conditions of Theorem 1. Moreover, an important property, which proof can be found in [Rawlings et al., 2017], states that upon satisfaction of the former conditions, the optimal cost sets an upper bound on the infinite-horizon cost along the resulting trajectory.

Corollary 1 *Given the dynamical system (3), the optimization problem (4) and the equilibrium set* $X^* \subseteq \mathbb{X}$*, if conditions 1.-6. of Theorem 1 are satisfied, then*

$$V_N^0(x_0) \leq \sum_{n=0}^{\infty} l(x(n), \kappa_N(x(n))), \tag{7}$$

holds $\forall x_0 \in \mathcal{X}_N$ *and* $x(n+1) = f(x(n), \kappa_N(x(n)))$.

This result implies, in the COVID-19 application case, that the resulting optimal cost is an upper bound on the minimum number of deaths that can be achieved at the end of the pandemic.

3.2 MPC-based vaccination for COVID-19 pandemic

The aim of the age-structured MPC vaccination strategy is to determine, at each sampled step (every day in the context of this work), the number of individuals from each age group to be vaccinated to minimize the death toll at the end of the pandemic. Here, the number of vaccines administered daily should not exceed the daily vaccination capacity, denoted $\bar{v}$. The ability of MPC to handle constraints makes it well suited for this task. Therefore, the ideal cost to be minimized, given as the summation of the daily number of deceased individuals, is represented as follows:

$$\lim_{n \to +\infty} \sum_{k=1}^{n_a} D_k(n) = \sum_{n=0}^{\infty} \sum_{k=1}^{n_a} D_k(n+1) - D_k(n) = \sum_{n=0}^{\infty} \sum_{k=1}^{n_a} \gamma_{D_k} I_k(n) = \sum_{n=0}^{\infty} \gamma_D^\top I(n) \tag{8}$$

Since it is not possible to solve the infinite-horizon optimal control problem, the MPC approach is employed. The stage cost of the MPC serves as an upper bound for (8), and is defined as the daily number of deceased individuals: $l(x(n), u(n)) = \gamma_D^\top I(n)$. Additionally, an appropriate final cost is incorporated. The final cost is derived from a local Lyapunov function, defined within the invariant set $\mathbb{X}_f$, as illustrated in Theorem 2.

Theorem 2 *Given the discrete-time dynamics in (2) and the optimization problem in (4) with* $x = (S, I, R, D) \in \mathbb{R}^{4n_a}$*, the population in every age group* $P \in \mathbb{R}^{n_a}$*, supposed to be constant in time, and*

$$\mathbb{X} = \{x \in \mathbb{R}^{4n_a} : 0 \leq S \leq P,\ 0 \leq I \leq P,\ 0 \leq R \leq P,\ 0 \leq D \leq P\}, \tag{9}$$

$$\mathbb{U} = \{u \in \mathbb{R}_a^n : u \geq 0,\ \sum_{k=1}^{n_a} u_k \leq \bar{v}\}, \qquad \mathbb{Z} = \mathbb{X} \times \mathbb{U}, \qquad X^* = \{x \in \mathbb{X} : I = 0\}. \tag{10}$$

Let $l(\cdot,\cdot), V_f(\cdot)$ and X_f be given by:

$$l(x(n),u(n)) = \gamma_D^\top I(n), \tag{11}$$

$$V_f(x(N)) = \frac{1}{\epsilon}\gamma_D^\top I(N) \tag{12}$$

$$\mathbb{X}_f = \{x \in \mathbb{X} : C^\top \Lambda S \leq \Gamma\} \cup X^*, \tag{13}$$

where

$$C = \begin{pmatrix} C_{11} & \cdots & C_{1n_a} \\ \vdots & \ddots & \vdots \\ C_{n_a1} & \cdots & C_{n_an_a} \end{pmatrix}, \ \Lambda = \begin{pmatrix} \gamma_{D_1}\lambda_1 & \cdots & 0 \\ \vdots & \ddots & \vdots \\ 0 & \cdots & \gamma_{D_{n_a}}\lambda_{n_a} \end{pmatrix}, \ \Gamma = \begin{pmatrix} \gamma_{D_1}(\gamma_{R_1}+\gamma_{D_1}-\epsilon) \\ \vdots \\ \gamma_{D_{n_a}}(\gamma_{R_{n_a}}+\gamma_{D_{n_a}}-\epsilon) \end{pmatrix} \tag{14}$$

with $\epsilon \in \mathbb{R}$ such that $0 < \epsilon < \min_{k=1,\ldots,n_a}\{\gamma_{R_k}+\gamma_{D_k}\}$.
Then, the following assertions hold:

i. $\forall x \in \mathcal{X}_N$, there exists a solution $\mathbf{u}^0$ to the optimal control problem in (4);

ii. the set X^* is asymptotically stable in $\mathcal{X}_N$ for $x(n+1) = f(x(n), \kappa_N(x(n)))$;

iii. the optimal value $V_N^0(x)$ is an upper bound for the total number of future deceased individuals if the MPC control $\kappa_N(x)$ is applied.

Proof 1 *Assertions* i. *and* ii. *are proved by showing that the six conditions of Theorem 1 are satisfied.*

1.-2.-3. *By definition, the sets $\mathbb{X}$, $\mathbb{U}$, $\mathbb{Z}$, X^* and $\mathbb{X}_f$ and the functions $l(\cdot,\cdot)$, $f(\cdot)$ and $V_f(\cdot)$ satisfy conditions* 1, 2, *and* 3 *of Theorem* 1.

4. *First note that X^* is invariant $\forall u \in \mathbb{U}$ since no one can get infected if there are no infected individuals. Consider the condition under which the daily sum of deceased individuals is decreasing $\forall u \in \mathbb{U}$, such that:*

$$\gamma_D^\top I(n+1) - \gamma_D^\top I(n) \leq -\epsilon\gamma_D^\top I(n) \tag{15}$$

with $0 < \epsilon < \min_{k=1,\ldots,n_a}\{\gamma_{R_k}+\gamma_{D_k}\}$.
From the discrete-time dynamics in (2), condition (15) can be represented as follows:

$$\begin{aligned} &\sum_{k=1}^{n_a}\gamma_{D_k}\lambda_k S_k(n)\sum_{j=1}^{n_a}C_{k,j}I_j(n) - \sum_{j=1}^{n_a}\gamma_{D_j}(\gamma_{R_j}+\gamma_{D_j}-\epsilon)I_j(n) \leq 0 \\ \iff &\sum_{j=1}^{n_a}\left(\sum_{k=1}^{n_a}\gamma_{D_k}\lambda_k S_k(n)C_{k,j} - \gamma_{D_j}(\gamma_{R_j}+\gamma_{D_j}-\epsilon)\right)I_j(n) \leq 0. \end{aligned} \tag{16}$$

Note that the one-step decreasing condition does not depend on the input. From the non-negativity of the number of infected individuals $I(n)$, condition (16) is satisfied if (17) holds.

$$\sum_{k=1}^{n_a}\gamma_{D_k}\lambda_k S_k(n)C_{k,j} \leq \gamma_{D_j}(\gamma_{R_j}+\gamma_{D_j}-\epsilon), \quad \forall j = 1,\ldots,n_a \tag{17}$$

The term in (17) is given in matrix form by $C^\top\Lambda S(n) \leq \Gamma$, see (13) and (14). Moreover, from the non-increasing nature of the number of susceptible individuals $S(n)$ and the positivity of matrices C and Λ, it follows that $C^\top\Lambda S(n+1) \leq C^\top\Lambda S(n) \leq \Gamma$. Hence, (13) is an invariant set of the system $\forall u \in \mathbb{U}$, satisfying condition 4.(a). *To prove the satisfaction of condition* 4.(b), *note that (18) holds $\forall x \in \mathbb{X}_f$.*

$$V_f(f(x,0)) - V_f(x) = \frac{1}{\epsilon}(\lambda_D^\top I^+ - \lambda_D^\top I) \leq -\lambda_D^\top I = -l(x,0) \tag{18}$$

5. *Consider* $x \in \mathcal{X}_N$ *and* $u \in \mathcal{U}_N$ *such that* $(x,u) \in \mathbb{Z}$. *By defining* $\underline{\gamma_D} = \min_{k=1,\dots,n_1} \gamma_{D_k}$, *which is positive by construction, it follows that:*

$$l(x,u) = \gamma_D^\top I \geq \underline{\gamma_D} \sum_{k=1}^{n_a} I_k = \underline{\gamma_D} \|I\|_1 = \underline{\gamma_D} \|x\|_{X^*}.$$

Then, condition 5.(a) *holds with* $\alpha_1(y) = \underline{\gamma_D} y$ *of class* $\mathcal{K}_\infty$. *Condition* 5.(b) *holds with* $\alpha_f(y) = \frac{1}{\epsilon}\bar{\gamma}_D y$ *of class* $\mathcal{K}_\infty$, *where* $\bar{\gamma}_D = \max_{k=1,\dots,n_a} \gamma_{D_k}$.

6. *From the discrete-time SIRD model in (2), it follows that*

$$\gamma_D^\top I(n+1) = \gamma_D^\top (\mathbb{I} + S_d(n)\Lambda C - \Gamma_{RD}) I(n)$$

where $\mathbb{I}$ *is an identity matrix of dimensions* $n_a \times n_a$, *and*

$$S_d = \begin{pmatrix} S_1 & & \\ & \ddots & \\ & & S_{n_a} \end{pmatrix}, \quad P_d = \begin{pmatrix} P_1 & & \\ & \ddots & \\ & & P_{n_a} \end{pmatrix}, \quad \Gamma_{RD} = \begin{pmatrix} \gamma_{R_1} + \gamma_{D_1} & & \\ & \ddots & \\ & & \gamma_{R_{n_a}} + \gamma_{D_{n_a}} \end{pmatrix}.$$

From the bounds on the number of infected and susceptible individuals at every step n, *it follows that* $0 \leq S(n) \leq P$, *where* P *is the total population in every age group. Moreover, from the positivity of* Λ *and* C, *it implies that*

$$\gamma_D^\top I(n+1) = \gamma_D^\top (\mathbb{I} + S_d(n)\Lambda C - \Gamma_{RD}) I(n) \leq \gamma_D^\top (\mathbb{I} + P_d \Lambda C - \Gamma_{RD}) I(n) \leq \eta \gamma_D^\top I(n) \tag{19}$$

for $\eta > 0$, *where* η *is big enough. From (12) and (19), it follows that:*

$$\begin{aligned} &\gamma_D^\top I(n+i) \leq \eta^i \gamma_D^\top I(n), \quad \forall n \in \mathbb{N}, i \in \mathbb{N} \\ &V_f(x(n+N)) = \frac{1}{\epsilon}\gamma_D^\top I(n+N) \leq \frac{1}{\epsilon}\eta^N \gamma_D^\top I(n), \quad \forall I(n) \in \mathbb{R}_+^n, N \in \mathbb{N}, \end{aligned}$$

which extends to:

$$\begin{aligned} V_N^0(x(n)) &= \sum_{i=0}^{N-1} \gamma_D^\top I(n+i) + V_f(x(n+N)) \leq \left(\epsilon^{-1}\eta^N + \sum_{i=0}^{N-1} \eta^i\right) \gamma_D^\top I(n) \\ &\leq \left(\epsilon^{-1}\eta^N + \sum_{i=0}^{N-1} \eta^i\right) \|\gamma_D\|_1 \|I(n)\|_1 = \left(\epsilon^{-1}\eta^N + \sum_{i=0}^{N-1} \eta^i\right) \|\gamma_D\|_1 \|x(n)\|_{X^*} \end{aligned} \tag{20}$$

This indicates that the bound in condition 6. *holds with* $\alpha(y) = \left(\epsilon^{-1}\eta^N + \sum_{i=0}^{N-1} \eta^i\right) \|\gamma_D\|_1 y$.

Finally, Assertion iii. *is a direct consequence of Corollary 1.*

3.3 MPC-based vaccination implementation

To implement the MPC vaccination strategy, it is essential to gather data on the number of infected and deceased individuals at each sampled step. In the context of this work, the vaccination strategy requires daily data acquisition to update the initial states of the discrete-time model in (2) used inside the MPC. This enables the MPC to compute the daily number of vaccines to be administered per age group over the vaccination strategy horizon, N_v. The MPC structure is illustrated in Algorithm 1.

Recall that the equilibrium set is defined as $X^* = \{x \in \mathbb{X} : I = 0\}$, and note that neither the problem constraints nor the cost function depend on the recovered or past deceased populations. In fact, the cost in (8) representing the sum of future deaths depends only on susceptible and infected populations. This implies that the solution of the MPC problem is not affected by the dynamics of D and R. Then, a reduced-order dynamical model can be employed inside the MPC. Hence, the state vector representing the daily number of susceptible and infected individuals in each age group can be defined as $x = (S, I) \in \mathbb{X}$, where

$$\begin{aligned} \mathbb{X} &:= \{x = (S,I) \in \mathbb{R}^{2n_a} : 0 \leq S \leq P, \quad 0 \leq I \leq P\}, \\ X^* &:= \{x = (S,I) \in \mathbb{R}^{2n_a} : I = 0\}. \end{aligned}$$

Algorithm 1 MPC Vaccination Strategy

Define the MPC parameters: the prediction horizon N, the vaccination strategy horizon N_v, the maximum daily vaccination capacity $\bar{v}$, and the threshold on infected population to determine pandemic eradication $I_e \in \mathbb{R}^{n_a}$;
Define the initial states and populations: $S_k(0)$, $I_k(0)$, $R_k(0)$, $D_k(0)$ and P_k $\forall k \in \{1, 2, \ldots, n_a\}$;
for each day $n = 0, 1, \ldots, N_v$ **do**
    Obtain the current state values $S_k(n)$, $I_k(n)$, $R_k(n)$ and $D_k(n)$;
    if $I_k(n) \leq I_e$ **then**
        The disease is eradicated: stop vaccinating;
    else
        Solve the optimization problem in (4) with (9)-(14);
        Extract the first element of the optimal control sequence: $\kappa_N(x_k(n)) = u_k^0(0, x_k(n))$;
        Administer vaccines according to $u_k(n) = \kappa_N(x_k(n))$;
    end if
    Update the state;
end for

Here, $\mathbb{X}$ and X^* represent the projections of the full state sets onto the subspace of susceptible and infected populations. Consequently, the MPC problem can be equivalently expressed in their terms, simplifying the optimization problem while preserving the essential dynamics.

4 Results and Discussion

To demonstrate the effectiveness of the MPC vaccination strategy, it is necessary to compare its performance with both the strategy adopted by the Belgian government during the first wave of vaccination and the no vaccination approach. This analysis uses the model in (2) to forecast the demographic consequences of the three proposed scenarios on the Walloon population.

4.1 Simulation parameters

To simulate the impact of a vaccination strategy on a given population, it is crucial to gather enough demographic information to represent it. To start, the data are categorized into $n_a = 6$ different age groups with respective populations P_k for $k \in \{1, 2, \ldots, n_a\}$. The Walloon population per age group is obtained from the website of the Belgian statistical office [Statbel, 2018]. The maximum number of vaccines administered during a single day in Wallonia is $\bar{v} = 55191$ shots, which occurred on June 16, 2021 [Sciensano, 2020]. This number is used to set the threshold for the daily vaccination capacity. The contact matrix C_{kj} is obtained using the online tool Socrates (social contact rates) [Willem et al., 2020]. For this work, data collected from Belgium in 2010 are used. The elements of the social contact matrix are divided by the total number of individuals in each age group to adjust it to the Walloon population. The remaining simulation parameters: λ_k, γ_{R_k}, γ_{D_k}, and the initial number of infected individuals I_{0_k} are obtained from [Sonveaux, 2023], where the author used a genetic algorithm to calibrate the model parameters in (1) using data from Wallonia. No drugs are administered and no cases of deceased or recovered individuals are recorded prior to the simulation. The simulation time is set to $t_{sim} = 140$ *days*. The simulation time is equivalent to the vaccination strategy horizon, N_v. The simulation parameters are summarized in Table 1.

4.2 No vaccination strategy

At the beginning of every epidemic, a fundamental question arises: is vaccination necessary? The primary goal of vaccination is to reduce the severe effects and limit the spread of viruses and diseases. However, some might argue that the immune system of humans is capable of adapting to and defeating new diseases. In the case of COVID-19, a notable number of deaths have been reported among individuals with weak immunity and pre-existing comorbidity. To forecast the demographic consequences of

k	*range*	P_k	λ_k	γ_{R_k}	γ_{D_k}	I_{0_k}
1	0-24	1058304	0.0769924521	0.9216927886	0.0004407167	4.6595088243
2	25-44	0915796	0.0290873349	0.7230105996	0.0018303543	4.3296088874
3	45-64	0983789	0.0136872530	0.5707245171	0.0232746601	4.8417769521
4	65-74	0384803	0.1149749309	0.8482912034	0.0397484004	0.1709101349
5	75-84	0203035	0.2326289564	0.8200428486	0.1006921381	1.4936938584
6	85+	0099516	0.3331837058	0.6612236351	0.1514435560	1.6144863665

Table 1: Age-structured SIRD model simulation parameters

choosing not to vaccinate the Walloon population, the evolution of population dynamics is simulated using the model in (2) with zero input.

Graphically, Figure 3 illustrates the evolution of population dynamics over time when no vaccine is administered. Figure 3b shows that the disease does not eradicate within the specified simulation time, while Figure 3d depicts the intolerable growth in the COVID-19 death toll. When no vaccine is administered, more than 16% of the Walloon population becomes infected, with a total death toll of 15497 individuals during the simulation period. In summary, these alarming findings underscore the urgent need for an effective vaccination strategy to minimize deaths.

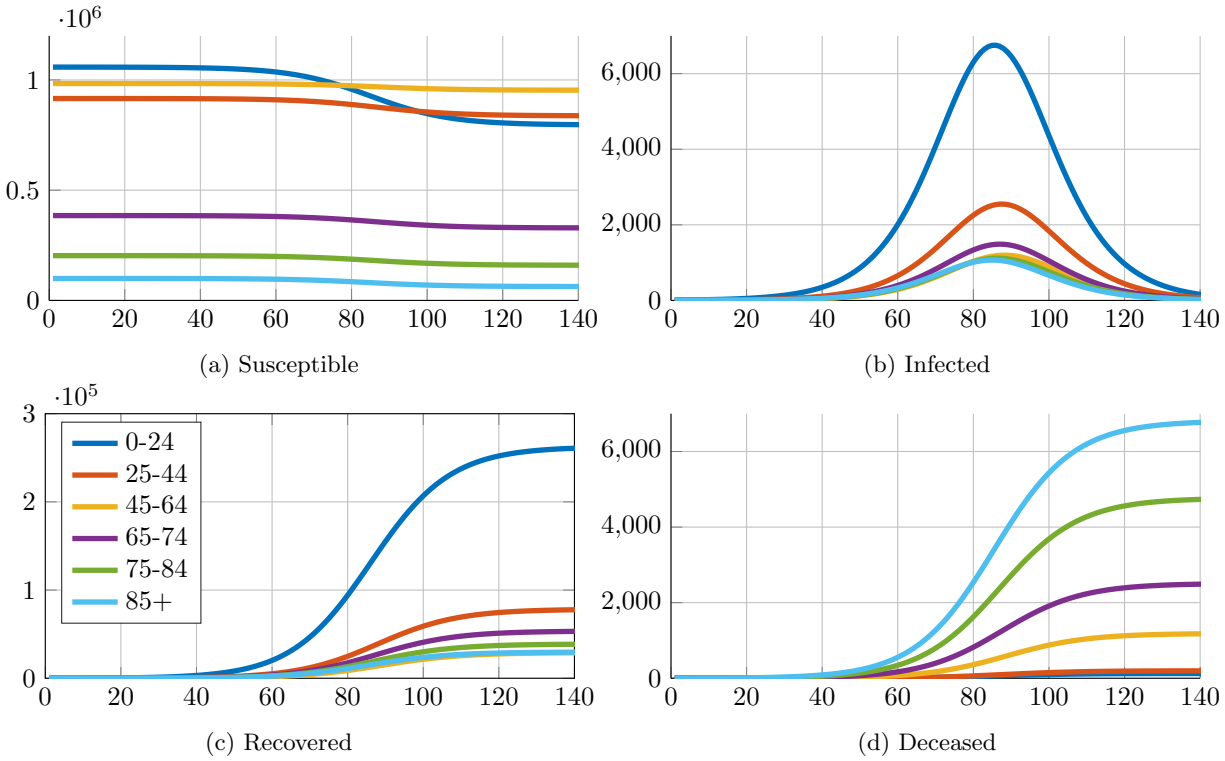

(a) Susceptible

(b) Infected

(c) Recovered

(d) Deceased

Figure 3: Populations evolution over time (in days) in the absence of vaccination

4.3 National vaccination strategy

During the first wave of vaccination, decision makers in Belgium adopted a decreasing age strategy to limit virus transmission and save as many lives as possible. Given that COVID-19 has been shown to be more fatal in older age groups, the national strategy prioritizes vaccinating the elderly first, then progressively moving to younger age groups. The objective of this hierarchical approach is to first drive the number of susceptible individuals in the oldest age group to zero before moving down the age hierarchy, systematically covering the whole population until the disease is eradicated. Here, disease eradication is defined as $I_{e,k} < 1$ for all $k \in \{1, 2, \ldots, n_a\}$.

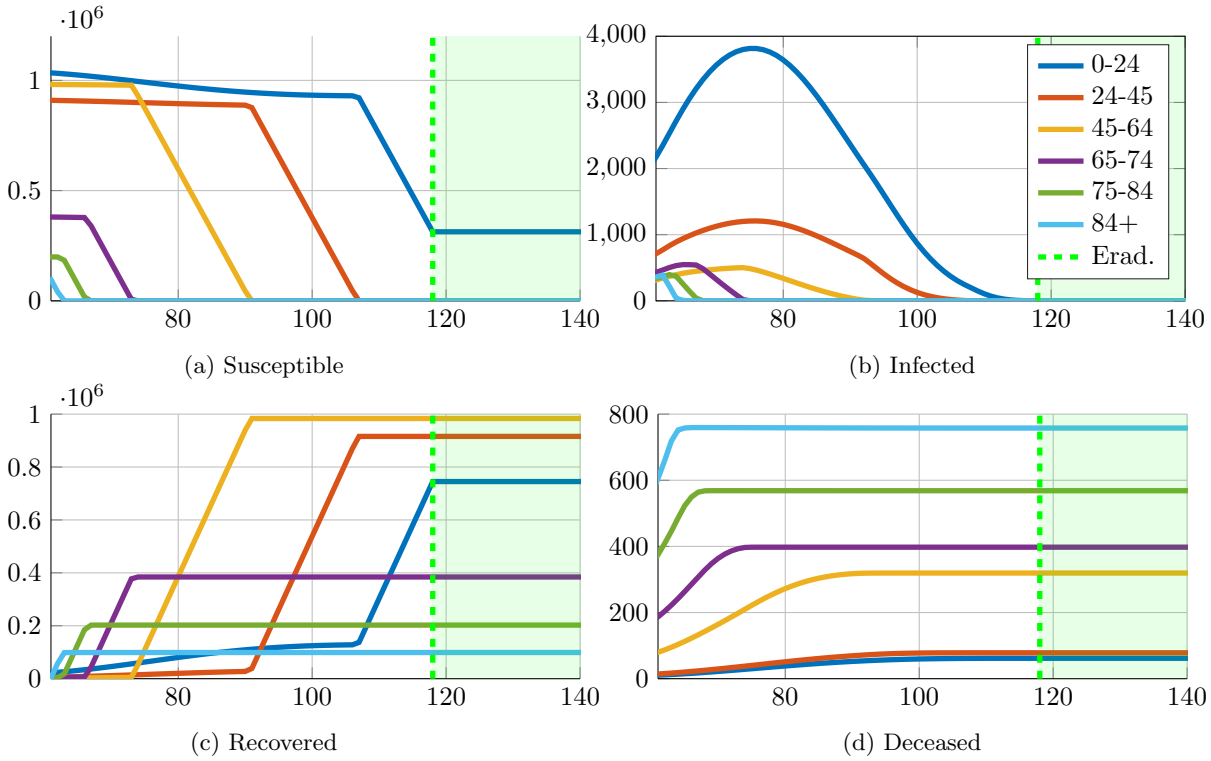

(a) Susceptible

(b) Infected

(c) Recovered

(d) Deceased

Figure 4: Populations evolution over time (in days) under the national vaccination strategy

To comply with realistic settings, the national vaccination strategy is implemented two months after the COVID-19 outbreak, assuming that this is the period required for the development and testing of the vaccine. In Figure 4b, it is shown that the disease is eradicated within 57 days from the start of vaccination. In addition, the fraction of infected individuals decreases dramatically to 5.96% after vaccination. Figure 4d highlights a significant reduction in the total death toll since the beginning of vaccination, which decreases by 79.9% under the national strategy compared to no administration. The green-shaded area represents the safe zone: the period of time during which the disease is no longer present. A larger safe zone indicates faster disease eradication.

Despite its benefits, the national vaccination strategy is not optimal in terms of the final death toll, as shown in the following sections. Moreover, the decreasing age approach does not account for additional factors, such as exposure levels and pandemic spreading rates. As proved in the following, taking explicitly into account the pandemics dynamics allows to develop a more advanced strategy capable of further reducing the final death toll, eradicating the disease faster while consuming fewer vaccines.

4.4 MPC vaccination strategy

An MPC vaccination strategy aimed at minimizing deaths is proposed here, with the goal of developing a systematic and optimal strategy to vaccinate the Walloon population while adhering to operational constraints. The MPC algorithm is summarized in Algorithm 1. The values of the MPC parameters used for this simulation are $N = 40$ days and $\epsilon = 0.1$.

As for the former approach, the MPC is tested following the availability of vaccines: two months after the COVID-19 outbreak. Figure 5 illustrates the demographic improvements using the MPC approach. In Figure 5b, the eradication time decreases to 37 days from the beginning of vaccination, and the fraction of infected individuals is reduced to 3.67%. Consequently, the total disease death toll since the beginning of vaccination in Figure 5d decreases by 80.3% under the MPC strategy compared to the absence of administration. This improvement is attributed to the model-based nature of the MPC. The MPC uses the mathematical model in (2) to guide its decisions, incorporating information such as contact, death, and recovery rates for each age group. This represents an improvement over the national strategy, which solely bases its decisions on age.

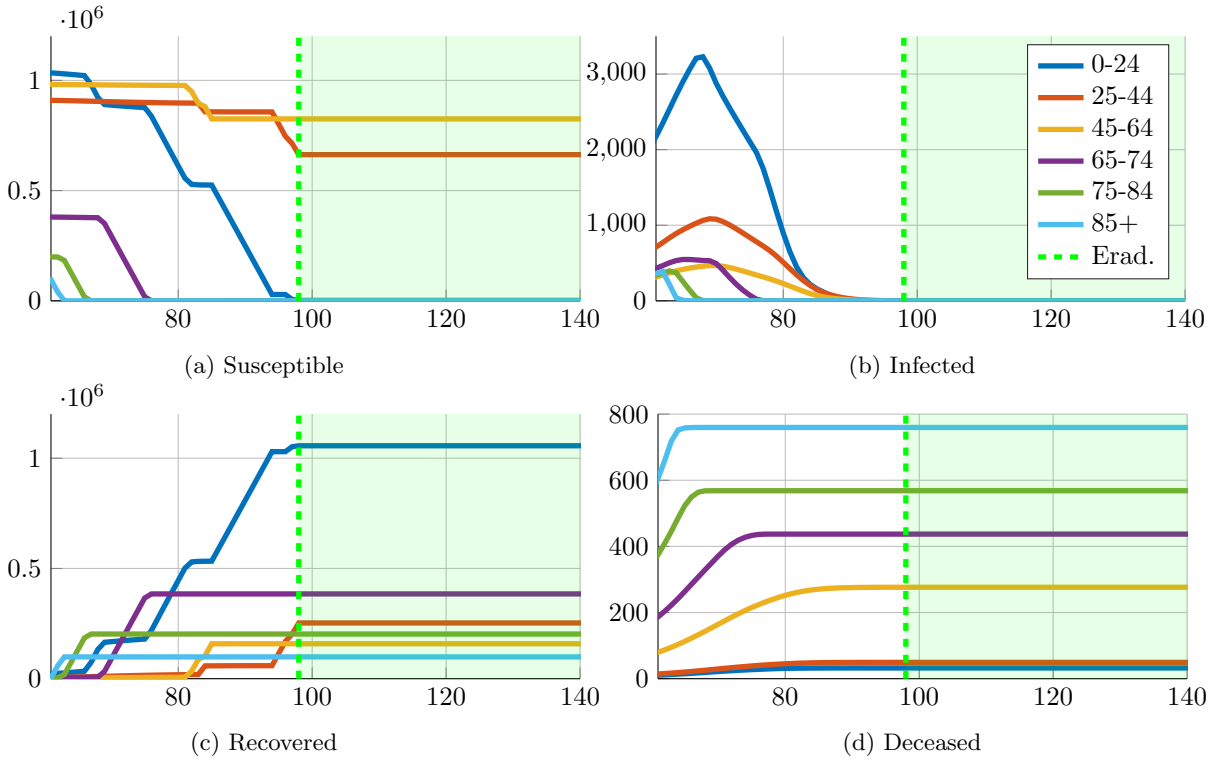

(a) Susceptible (b) Infected

(c) Recovered (d) Deceased

Figure 5: Populations evolution over time (in days) under the MPC vaccination strategy

	Deceased	Infected	Eradication	Injected Vaccines
National Strategy	911	169578	57 days	3145887
MPC Strategy	851	86314	37 days	2042017
Improvement	6.6%	49.1%	35.1%	35.1%

Table 2: Statistical comparison between the national and the MPC vaccination strategies

4.5 Discussion

Comparing both vaccination strategies, Figure 6 demonstrates that the MPC provides an improved performance in eradicating the disease and saving as many lives as possible. Graphically, the safe zone occupies a significantly larger area in Figure 6b compared to Figure 6a. A larger safe zone is equivalent to faster disease eradication time. Numerically, it can be concluded that the MPC approach is 35% faster than the national strategy in eradicating the disease. This results in the MPC decreasing the total number of infected individuals by 49% compared to the national strategy. Moreover, since vaccination is carried out daily at maximum capacity, the speed of disease eradication is inversely proportional to the number of vaccines consumed. This suggests that the MPC approach is more cost effective than the national strategy, as it requires 35% fewer vaccines to achieve disease eradication. Furthermore, while not graphically prominent in Figure 6, the MPC approach saves 6.6% more lives compared to the national strategy. Ethically, this alone establishes the MPC as the preferred method. The offset in the total number of deceased individuals between the two approaches is better represented in Figure 8. Their respective performance is summarized in Table 2.

In terms of vaccination, Figure 7 illustrates the significant difference between the two approaches. The national strategy in Figure 7a follows a decreasing age approach. This strategy prioritizes vaccination of the older age groups. In contrast, the MPC strategy in Figure 7b employs a more dynamic approach. The MPC strategy allows to simultaneously vaccinate multiple age groups at once. This stems from the model-based nature of the MPC that accounts for different factors to take its decisions. Consequently, the MPC is better also for minimizing deaths compared to the national strategy.

As previously mentioned, the MPC approach requires 35% fewer vaccines compared to the national

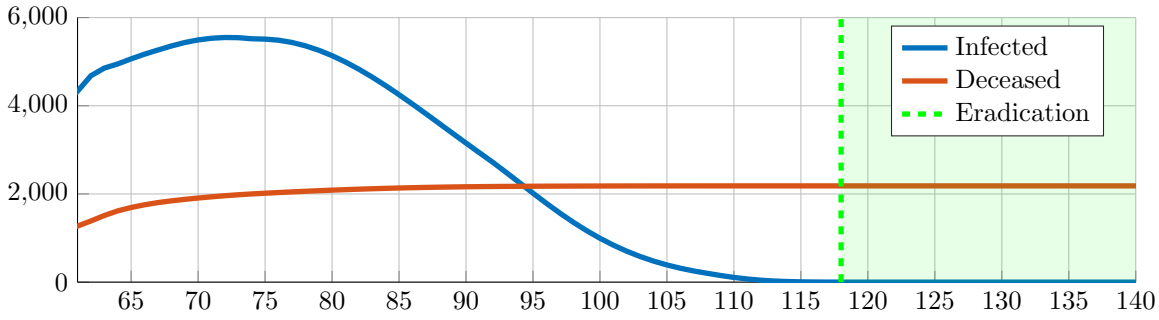

(a) National vaccination strategy

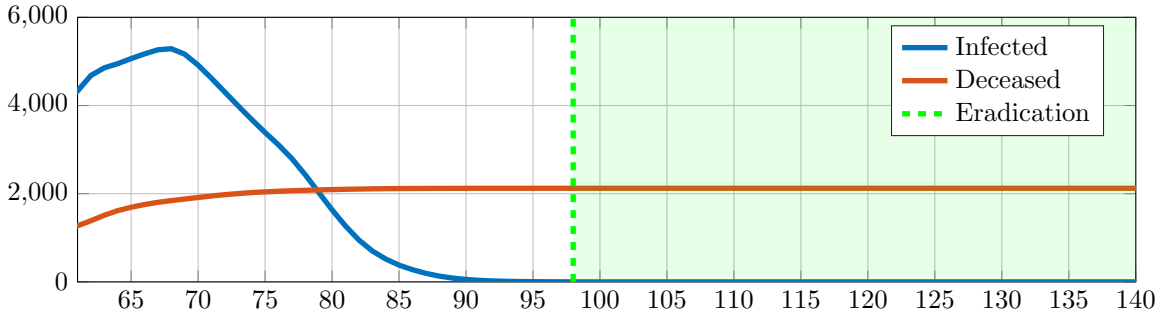

(b) MPC vaccination strategy

Figure 6: Daily infected and total deceased evolution over time (in days)

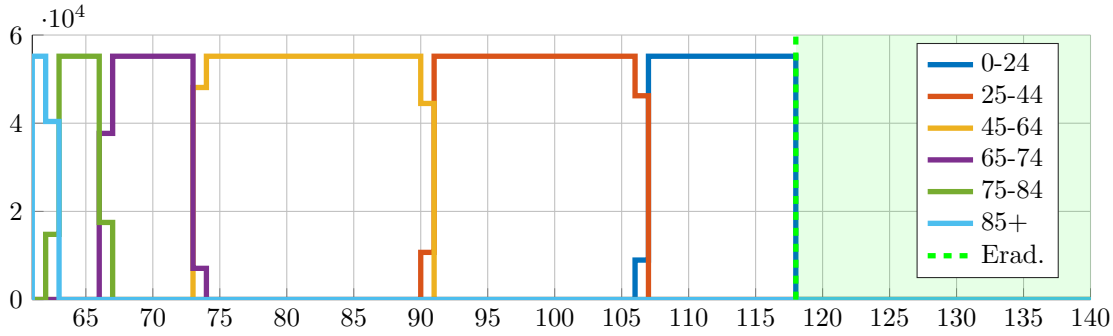

(a) National vaccination strategy

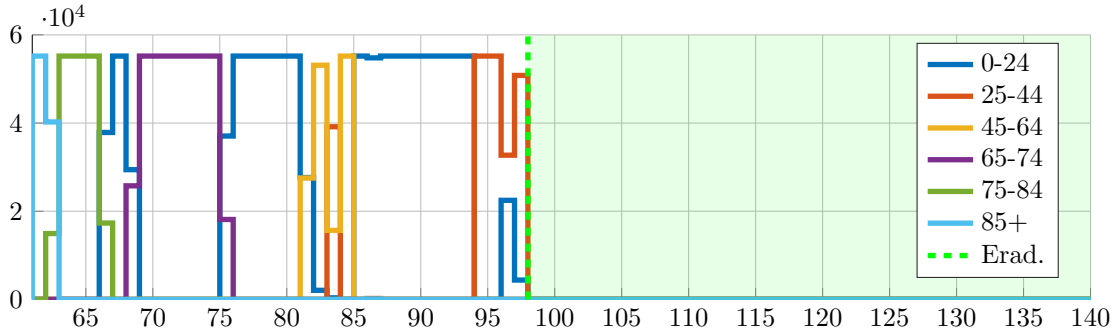

(b) MPC vaccination strategy

Figure 7: Vaccine administration evolution over time (in days)

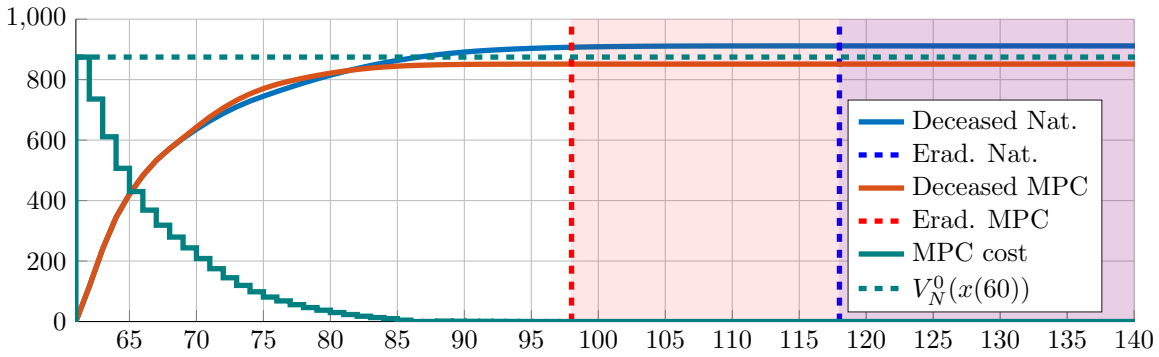

Figure 8: Evolution of the MPC cost versus the total number of deceased individuals under the MPC and national strategies since the start of vaccination until disease eradication

strategy to achieve disease eradication. This gives the MPC its cost-effective characteristics, making it suitable for implementation in nations with weak economies. Moreover, Figure 8 highlights the performance improvement of the proposed MPC approach, providing a comparison of the evolution of the total death toll after vaccine administration using both strategies. Note moreover that, as expected from Theorem 2, the MPC results in a final death toll that is upper-bounded by the MPC cost, whereas the national strategy violates such upper bound. Indeed, the MPC cost in Figure 8 is an upper bound for the minimum overall number of deaths achievable at the end of the simulation. In addition, it is interesting to note that the MPC-based strategy temporarily generates a higher number of deceased individuals, see values around day 75, although the final death toll is lower than that obtained under the national strategy. This counterintuitive observation confirms that the design of the optimal vaccination strategy is not a trivial problem to be addressed.

5 Conclusion

In this work, a novel Model Predictive Control (MPC) approach is proposed to develop an optimal age-structured vaccination strategy for the first wave of COVID-19, with the primary objective of minimizing deaths. The key contribution of this work lies in providing a detailed proof of the recursive feasibility and asymptotic stability of the proposed MPC algorithm. Through comprehensive simulations, it was demonstrated that the MPC approach outperforms the decreasing age vaccination strategy employed by the Belgian government. Specifically, the MPC strategy results in fewer deaths, fewer infections, faster disease eradication, and more efficient vaccine distribution.

The strength of the MPC approach comes from its predictive capability, which allows it to dynamically adjust to changing conditions, and its model-based nature, which integrates different factors such as contact rates, death rates, and recovery rates across different age groups. Moreover, the proposed MPC framework is not limited to COVID-19. Different models can be used to adapt the proposed strategy to different epidemics. This flexibility enables rapid deployment as soon as vaccines become available. In addition, advances in modeling and data science can benefit the proposed MPC approach by improving the predictive accuracy of the integrated model.

Furthermore, it is assumed that the vaccine exhibits perfect efficacy in this study. In reality, the effectiveness of vaccination is not necessarily absolute [Braeye et al., 2022]. Future work will account for this issue by introducing a parameter to model the efficacy of the vaccine for each age group. It will also incorporate additional constraints, such as the capacity of the daily ICU (Intensive Care Unit), to assess how the MPC adjusts its decisions to satisfy different operational conditions.

Acknowledgments

- Computational resources have been provided by the Consortium des Équipements de Calcul Intensif (CÉCI), funded by the Fonds de la Recherche Scientifique de Belgique (F.R.S.-FNRS) under Grant No. 2.5020.11 and by the Walloon Region.

- The "AVIQ, l'Agence Wallonne pour la Santé, la Protection sociale, le Handicap et les Familles" has given access to valuable data for the calibration of the parameters.

Data availability

The sources of data and the parameters used are explicitly mentioned in the paper, allowing the reader to reproduce the simulations. The Python code can be made available upon request.

Funding

No specific funding is linked to this research.

Conflicts of interest

The authors declare that they have no conflict of interest.

Ethics declaration

The article process does not affect any humans, birds, or animals.

References

[Abrams et al., 2021] Abrams, S., Wambua, J., Santermans, E., Willem, L., Kuylen, E., Coletti, P., Libin, P., Faes, C., Petrof, O., Herzog, S. A., et al. (2021). Modelling the early phase of the Belgian COVID-19 epidemic using a stochastic compartmental model and studying its implied future trajectories. *Epidemics*, 35:100449.

[Alleman et al., 2021] Alleman, T. W., Vergeynst, J., De Visscher, L., Rollier, M., Torfs, E., Nopens, I., Baetens, J. M., et al. (2021). Assessing the effects of non-pharmaceutical interventions on SARS-CoV-2 transmission in Belgium by means of an extended SEIQRD model and public mobility data. *Epidemics*, 37:100505.

[Braeye et al., 2022] Braeye, T., van Loenhout, J., Brondeel, R., Stouten, V., Hubin, P., and Billuart (2022). COVID-19 vaccine effectiveness against symptomatic infection and hospitalization in Belgium, July 2021-April 2022. *Euro Surveill.*

[Brauer, 2008] Brauer, F. (2008). Compartmental models in epidemiology. *Mathematical epidemiology*, pages 19–79.

[Cartocci et al., 2021] Cartocci, A., Cevenini, G., and Barbini, P. (2021). A compartment modeling approach to reconstruct and analyze gender and age-grouped COVID-19 italian data for decision-making strategies. *Journal of Biomedical Informatics*, 118:103793.

[Davies et al., 2020] Davies, N. G., Klepac, P., Liu, Y., Prem, K., Jit, M., and Eggo, R. M. (2020). Age-dependent effects in the transmission and control of COVID-19 epidemics. *Nature medicine*, 26(8):1205–1211.

[Fiacchini and Alamir, 2021] Fiacchini, M. and Alamir, M. (2021). The Ockham's razor applied to COVID-19 model fitting French data. *Annual Reviews in Control*, 51:500–510.

[Franco, 2021] Franco, N. (2021). COVID-19 Belgium: Extended SEIR-QD model with nursing homes and long-term scenarios-based forecasts. *Epidemics*, 37:100490.

[Grundel et al., 2022] Grundel, S., Heyder, S., Hotz, T., Ritschel, T. K., Sauerteig, P., and Worthmann, K. (2022). How much testing and social distancing is required to control COVID-19? Some insight based on an age-differentiated compartmental model. *SIAM Journal on Control and Optimization*, 60(2):S145–S169.

[Kermack and McKendrick, 1991] Kermack, W. O. and McKendrick, A. G. (1991). Contributions to the mathematical theory of epidemics—II. The problem of endemicity. *Bulletin of mathematical biology*, 53(1-2):57–87.

[Morato et al., 2020] Morato, M. M., Bastos, S. B., Cajueiro, D. O., and Normey-Rico, J. E. (2020). An optimal predictive control strategy for covid-19 (sars-cov-2) social distancing policies in brazil. *Annual Reviews in Control*, 50:417–431.

[Parino et al., 2023] Parino, F., Zino, L., Calafiore, G. C., and Rizzo, A. (2023). A model predictive control approach to optimally devise a two-dose vaccination rollout: a case study on COVID-19 in Italy. *International journal of robust and nonlinear control*, 33(9):4808–4823.

[Rahmandad, 2022] Rahmandad, H. (2022). Behavioral responses to risk promote vaccinating high-contact individuals first. *System Dynamics Review*, 38(3):246–263.

[Rawlings et al., 2017] Rawlings, J. B., Mayne, D. Q., Diehl, M., et al. (2017). *Model predictive control: theory, computation, and design*, volume 2. Nob Hill Publishing Madison, WI.

[Sauerteig et al., 2022] Sauerteig, P., Esterhuizen, W., Wilson, M., Ritschel, T. K., Worthmann, K., and Streif, S. (2022). Model predictive control tailored to epidemic models. In *2022 European Control Conference (ECC)*, pages 743–748. IEEE.

[Sciensano, 2020] Sciensano (2020). COVID-19. epistat.

[Seborg et al., 2016] Seborg, D. E., Edgar, T. F., Mellichamp, D. A., and Doyle III, F. J. (2016). *Process dynamics and control*. John Wiley & Sons.

[Sonveaux, 2023] Sonveaux, C. (2023). *Dynamical analysis and feedback control of age-structured epidemic models*. Phd thesis, UNamur.

[Statbel, 2018] Statbel (2018). Structuur van de bevolking.

[Tolles and Luong, 2020] Tolles, J. and Luong, T. (2020). Modeling epidemics with compartmental models. *Jama*, 323(24):2515–2516.

[Willem et al., 2020] Willem, L., Van Hoang, T., Funk, S., Coletti, P., Beutels, P., and Hens, N. (2020). Socrates: an online tool leveraging a social contact data sharing initiative to assess mitigation strategies for COVID-19. *BMC research notes*, 13(1):293.

[World Health Organization, 2014] World Health Organization (2014). *Infection prevention and control of epidemic-and pandemic-prone acute respiratory infections in health care*. World Health Organization.

[World Health Organization, 2025] World Health Organization (2025). World health organization coronavirus (COVID-19) dashboard. Accessed: 2025-01-22.